(Received 31 October 2023, Accepted 9 March 2024, Scheduled 24 March 202)

Conformal Microstrip Antennas on the Rocket Cylinder

Anita Pascawati[1,*], Muh Fakhri[1], Aditya I. Wahdiyat[2], Idris E. Putro[1], Sonny D. Harsono[1], Mirza Z. Rahmat[1], Rahmat A. Duhri[1], Kandi Rahardiyanti[1], Herma Y. Irwanto[1], Yuyu Wahyu[3], Arief Rufiyanto[2], Budi Sulistya[2], Evi N. Qomariya[4], Cahyaning R. Rahayu[4], Rizki F. Ridho[4], and Muhammad R. K. Aziz[5]

[1] *Research Center for Rocket Technology, Research Organization for Aeronautics and Space National Research and Innovation Agency (BRIN), Rumpin, Bogor 16350, Indonesia*
[2] *Research Center for Electronics, Research Organization for Electronics and Informatics National Research and Innovation Agency (BRIN), Tangerang, Indonesia*
[3] *Research Center for Telecommunication, Research Organization for Electronics and Informatics National Research and Innovation Agency (BRIN), Bandung, Indonesia*
[4] *Politeknik Elektronika Negeri Surabaya (PENS), Surabaya, Indonesia*
[5] *Center for Intelligent Geolocation and Wireless Communications (iGlowcom), Electrical Engineering Institut Teknologi Sumatera (ITERA), Lampung Selatan, Indonesia*

ABSTRACT: This paper presents the design of conformal microstrip antennas wrapped around a rocket cylinder. These antennas should exhibit favorable S_{11}-parameter values within the desired radio frequency range and an omnidirectional radiation pattern. Given their external placement on rockets, the challenge in this context is to ensure heat resistance. Two types of conformal microstrip antennas are developed to address this issue: one features an 8×1 array of rectangular patch (RP) elements, and the other consists of a single long rectangular patch (LP) element. Each antenna is wrapped around the rocket cylinder, with the patch array elements tailored to match the cylinder circumference to achieve an omnidirectional radiation pattern. Both antennas operate at a resonant frequency of 2.44 GHz and are constructed using RT/duroid 5880, a flexible material with a low dielectric constant. The antenna designs are assessed through computer simulations, followed by fabrication and measurements to analyze their performance against simulation results. The results indicate that the conformal RP antenna displays an S_{11} value of -24.512 dB at the center frequency of 2.445 GHz featuring a 48 MHz bandwidth, while the conformal LP antenna discloses an S_{11} value of -16.76 dB at the center frequency of 2.44 GHz having a wider bandwidth of 55 MHz. Both of the conformal RP and LP antennas exhibit an omnidirectional radiation pattern with a maximum gain of 6.13 dB and 7.21 dB, respectively. Following simulation and testing results, the antennas can tolerate temperatures up to 71.8°C during flight tests. Although temperature variations trigger slight frequency shifts, these deviations are insignificant. Finally, the measurement results agree with the simulation ones.

1. INTRODUCTION

Rocket research plays a vital role not only in satellite launches but also in various other applications. Antennas are a critical component in rocket technology, serving the essential function of transmitting and receiving telemetry signals to establish communication between the rocket and ground stations. Furthermore, in the context of radio telemetry for rockets, these antennas relay essential data, such as the rocket coordinates from the global navigation satellite system (GNSS), information from attitude sensors, and video transmissions [1, 2]. While research on rocket antennas has been ongoing, only a few studies in the past decade have addressed specific types of rocket-mounted antennas, such as those placed inside the rocket nose cone [3, 4] and slotted antennas [5]. Other research focuses on antenna types suitable for mounting on the rocket cylindrical body, specifically blade antennas [6] and arrayed patch antennas [7, 8], which must withstand the heat generated during the rocket flight. These rocket antennas must exhibit an omnidirectional radiation pattern to ensure comprehensive signal coverage spanning 360° around the rocket.

Numerous microstrip antenna types have been suggested for rocket applications. Conformal microstrip antennas suit curved surfaces, including sounding rockets, space launchers, and airborne vehicles. [9] discusses the design of a multiband conformal microstrip antenna for the suborbital launcher, and [7] introduces a flush-mounted circumferential microstrip array antenna for sounding rockets. Moreover, [8] designs an arrayed patch of electrically small antennas (ESAs) mounted on a conducting cylinder, resulting in end-fire radiation patterns. In another study [2], a microstrip antenna using PEEK450G903 material is used for radio-interferometry on sounding rockets, operating in the 70 cm band with a 2.5 MHz bandwidth. Besides, ballistic rockets have been equipped with three types of antennas (wraparound, patch, and monopole) in [3]. Furthermore, concerning the investigation of a conformal antenna on various mediums, i.e., cylinder, cone, and spherical, several

* Corresponding author: Anita Pascawati (anita.pascawati@brin.go.id).

works employ Green's function technique. [10] conducts investigations aimed at resolving the spatial singularity problem present in the spectral domain Green's function for cylindrical multilayered media. [11] applies Green's function technique for an arbitrarily directed magnetic point source to enumerate slots on the spherical medium. In addition, [12] analyzes the input impedance and radiation pattern of the conical horn antenna using the development of Green's function. Moreover, [13] examines the use of multiple circular loop antennas on the conducting cone, resulting in a radiation pattern with the maximum values of E_θ at $\phi = 90°$ and weak at $\phi = 0°$. Then, [14] evaluates the effect of a loop antenna placed above the tip of the conducting cone to enhance signal transmission and minimize interference.

Several studies on microstrip array antennas have been conducted; however, they are primarily applied to 5G smartphone technologies. For instance, [15] designs a multiple input multiple output (MIMO) antenna featuring 18 slot elements with T-shaped feeding, providing a large bandwidth in sub-6-GHz LTE bands and ensuring the coupling isolation between elements. In [16], the design is enhanced with a 10 double-T based elements antenna, specifically aimed to achieve multi-band functionality in sub-6-GHz. Moreover, [17] evaluates an antenna with side edge eight loop elements to ensure effective isolation without the need for any decoupling structure.

This study proposes two conformal microstrip antennas, i.e., an antenna with 8×1 rectangular patch array elements [18] and an antenna with a single long rectangular patch element. Both are manufactured from Roger RT/Duroid 5880 material and operate at a 2.44 GHz center frequency. Furthermore, our proposed antennas are mounted on the rocket's outer body to avoid signal strength attenuation caused by the carbon nose cone. It is noteworthy that the simulation and fabrication results demonstrate the superiority of the proposed conformal antennas for applications in rocket communication systems: (1) They resonate in the 2.44 GHz frequency band of the employed radio transmitters, featuring a bandwidth ≥ 48 MHz; (2) the antennas mounted on the rocket cylinder exhibit omnidirectional radiation pattern with gain about ± 6 dB in the vertical polarization. Nevertheless, the antennas display a few side lobes with lower gain in the horizontal polarization. It should be noted that these antennas have already been utilized in our experimental rockets.

2. SYSTEM MODEL

A conformal microstrip antenna is a kind of antenna made of a Printed Circuit Board (PCB) having conductor layers as the radiator and the ground plane, also a particular substrate layer lying between the conductor layers. Specifically, the substrate material owns a certain dielectric constant, ϵ_r, and the determined thickness, h. Furthermore, a conformal microstrip antenna featuring several patch elements is designed by applying formulas deployed by [19]. The patch width (W_p) of the specified resonant frequency, f_r, is determined by

$$W_p = \frac{v_0}{2f_r\sqrt{\frac{\varepsilon_r+1}{2}}}, \tag{1}$$

where v_0 is the light speed in a vacuum. The patch length (L_p) is calculated by

$$L_p = \frac{v_0}{2f_0\sqrt{\varepsilon_{eff}}} - 0.824h\frac{(\varepsilon_{eff}+0.3)\left(\frac{W_p}{h}+0.264\right)}{(\varepsilon_{eff}-0.258)\left(\frac{W_p}{h}+0.8\right)}. \tag{2}$$

Moreover, with known values of W_p and L_p, the impedance of a patch antenna is determined by

$$R_{in} = 90\frac{(\varepsilon_r)^2}{\varepsilon_r - 1}\left(\frac{L_p}{W_p}\right). \tag{3}$$

In addition, the matching to 50 Ω of a patch antenna is applied by utilizing the inset feed (y_0) acquired from

$$R_{in}(y = y_0) = R_{in}\cos^2\left(\frac{\pi}{L_p}y_0\right). \tag{4}$$

Notably, the quarter wavelength transformers in the feeding network are employed in designing the patch antenna using

$$Z_f = \sqrt{Z_c R_{in}}. \tag{5}$$

Besides, the feeding network also applied several widths of particular impedance feed lines obtained from

$$Z_c = \begin{cases} \frac{60}{\sqrt{\varepsilon_{eff}}}\ln\left[\frac{8h}{W_0}+\frac{W_0}{4h}\right], & \frac{W_0}{h} \leq 1, \\ \frac{120\pi}{\sqrt{\varepsilon_{eff}}\left[\frac{W_0}{h}+1.393+0.667\ln\left(\frac{W_0}{h}+1.444\right)\right]}, & \frac{W_0}{h} > 1. \end{cases} \tag{6}$$

According to [20] and [21], for a conformal microstrip antenna with a single element of long rectangular patch, the patch width (W_p) can utilize the whole length of cylinder diameter. Meanwhile, the patch length (L_p) is calculated by

$$L_p = \frac{0.49\lambda}{\sqrt{\varepsilon_r}}. \tag{7}$$

Moreover, the number of feed points into the rectangular patch (N_f) should be greater than the number of wavelengths in the dielectric (W_d), as determined by

$$W_d = \frac{W_p\sqrt{\varepsilon_r}}{\lambda}, \tag{8}$$

where $N_f > W_d$. Furthermore, the admittance of rectangular patch is

$$G_a = \frac{\pi}{\lambda\eta}\left(1 - \frac{(ka)^2}{24}\right). \tag{9}$$

Since $\frac{(ka)^2}{24} \ll 1$, it is negligible and $\eta = 120\pi$ in vacuum, therefore

$$G_a = \frac{1}{120\lambda}, \tag{10}$$

or

$$R_a = 120\lambda, \tag{11}$$

and the resistance per unit width of the rectangular patch is expressed by

$$r_a = \frac{R_a}{W_p}. \tag{12}$$

Then, the input impedance (R_{in}) at the edge of the rectangular patch can be obtained from

$$R_{in} = \frac{r_a}{2}. \tag{13}$$

Since the rectangular patch is fed by N_f, R_{in} should be split into N_f feed points (Z_{in}). Therefore, the impedance of each feed point is calculated as

$$Z_{in} = N_f R_{in}. \tag{14}$$

Furthermore, the dielectric constants material and also the length of the radiation patch can be changed due to temperature variations (δT) which are expressed by [22]

$$\frac{\delta\varepsilon_r}{\varepsilon_r} = \alpha_{\varepsilon_r}\delta T, \tag{15}$$

$$\frac{\delta L_p}{L_p} = \alpha_L \delta T, \tag{16}$$

where α_{ε_r} and α_L represent thermal coefficient of dielectric material and coefficient thermal expansion, respectively. The frequency shift of the antenna δf_r is thus written as [22]

$$\delta f_r = -\frac{1}{2}\frac{\delta\varepsilon_r}{\varepsilon_r} f_r - \frac{\delta L_p}{L_p} f_r. \tag{17}$$

3. PROPOSED ANTENNA DESIGN

In this study, we propose two different kinds of conformal microstrip antennas, i.e., conformal microstrip rectangular patch array 8×1 (RP) antenna and conformal microstrip with a single long rectangular patch element (LP) antenna. Note that the *conformal* microstrip antenna is characterized as a *planar* microstrip antenna that is strategically positioned in a wrapped configuration around the cylindrical surface of a rocket. Both antennas function at the resonant frequency, denoted as f_r, of 2.44 GHz. It is noteworthy that both antennas employ identical material characteristics, i.e., RT/duroid 5880 substrates possessing a dielectric constant ϵ_r of 2.2 and a thickness h of 1.575 mm. The thickness of the top and bottom layers of copper, denoted as t, is 0.0175 mm. Furthermore, the design of these conformal microstrip antennas is accomplished by utilizing computer simulation technology (CST) software. The simulation assesses the S_{11}-parameter (also known as return loss), radiation pattern, gain, and additional antenna characteristics.

The proposed RP antenna consists of a configuration of eight rectangular patch elements organized in an array that spans the entirety of the antenna width, aligned with the diameter of the cylinder. The length and width of our proposed RP antenna are 160 mm and 609 mm, respectively. The rectangular patch of the RP antenna is configured in a width W_p of 50 mm and a length L_p of 41 mm, as determined from Equations (1) and (2), correspondingly. The arrangement of the rectangular patch array with dimensions of 8×1 elements is designed to achieve an omnidirectional radiation pattern. Subsequently, the spacing between the rectangular patch elements is determined as 0.6 times the wavelength (λ). This distance is configured to be greater than $\lambda/2$ to encompass the circumference of the cylinder, yet remain below one wavelength. This design aims to avoid the occurrence of mutual coupling, as observed in [19], which emphasizes that the spacing between elements is intended to remain below one wavelength to prevent the formation of multiple maximum lobes and should be equal to or less than $\lambda/2$ to prevent nulls. In addition, each rectangular patch element is interconnected through corporate feeding networks, ultimately converging into a single feed. Hence, the eight elements array is adjusted to enable the power divider of 2^n. Note that the feeding is applied by a SubMiniature version A (SMA) connector featuring an impedance of $50\,\Omega$. Furthermore, the utilization of an inset feed with a dimension of 10 mm is employed to facilitate the impedance matching of the antenna to $50\,\Omega$. This matching is determined by the calculations outlined in Equations (3) and (4). The design of the proposed RP antenna is shown in Fig. 1(a) for further elaboration.

In contrast, the design of the LP antenna employs a different methodology than the RP antenna. The length L_p and width W_p of our proposed LP antenna are 130 mm and 609 mm, respectively. The proposed LP antenna consists solely of a single element. Specifically, it utilizes a lengthy rectangular patch denoted as W_p that spans the entire circumference of the rocket cylinder. Moreover, the patch length L_p of 39.9 mm is derived from Equation (7). In the context of conformal form, it is necessary to establish the value of L_p as 39.5 mm, to get a frequency match of 2.44 GHz. Further elaboration on the subject matter is provided in the subsequent section. Nevertheless, the antenna also employs the corporate feeding networks with a specified number of feed points (N_f) calculated from (8). Thus, N_f should employ power divisions of 2^n. These feed points converge into a single input feed, using a $50\,\Omega$ SMA connector. It is important to note that the distance between feed points is determined by dividing W_p by $N_f + 1$. Fig. 1(b) illustrates the specific design details of the LP antenna.

Within the context of the feeding network, both conformal antennas utilize the corporate feeding network. This network is constructed by employing quarter wavelength transformers, as determined by Equation (5). Despite this, it employs a mix of many feed lines with different impedances. The feed lines possess varying widths, denoted as W_0, determined by their respective impedances, Z_c, which are computed using Equation (6). It is important to note that the selection of the corporate feeding network is based on the improvement of antenna gain [23]. The corporate feeding network in the RP antenna utilizes feed lines with characteristic impedances of $50\,\Omega$, $70.71\,\Omega$, and $100\,\Omega$, which have corresponding widths of 4.85 mm, 2.83 mm, and 1.41 mm, respectively. On the other hand, in addition to incorporating $50\,\Omega$, $70.71\,\Omega$, and $100\,\Omega$ feed lines, the LP antenna also employs feed lines featuring characteristic impedances of $96.91\,\Omega$, $48.46\,\Omega$, and $69.61\,\Omega$, with corresponding widths W_0 of 1.51 mm, 5.08 mm, and 2.86 mm, respectively. It should be

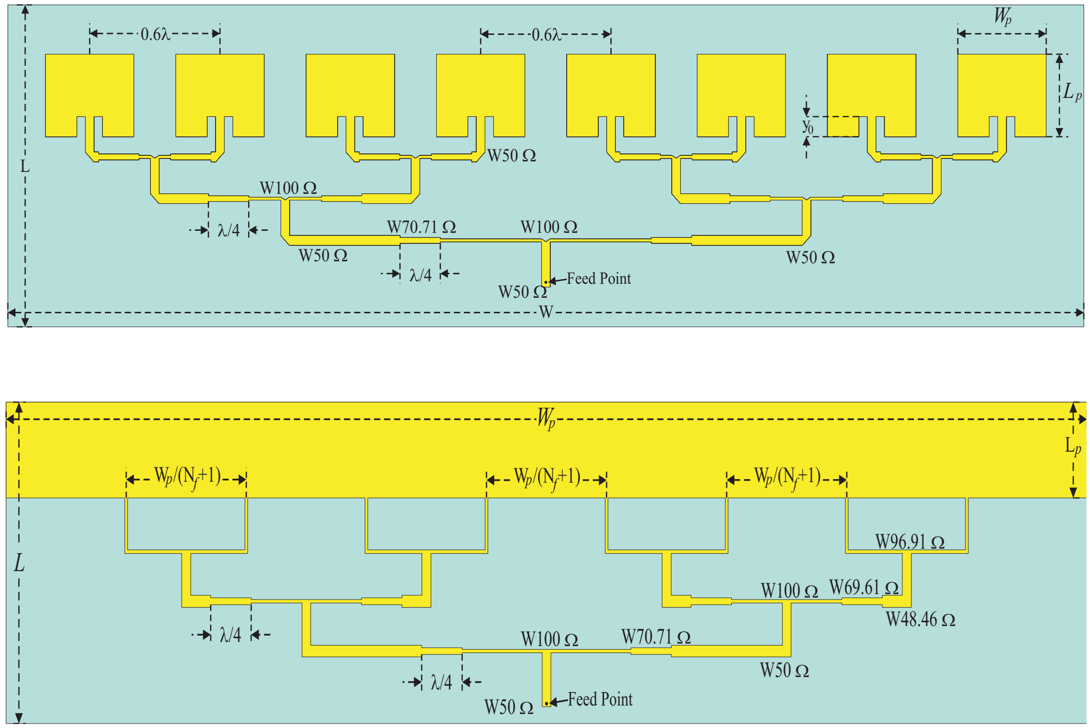

FIGURE 1. Design of planar antennas (a) RP and (b) LP.

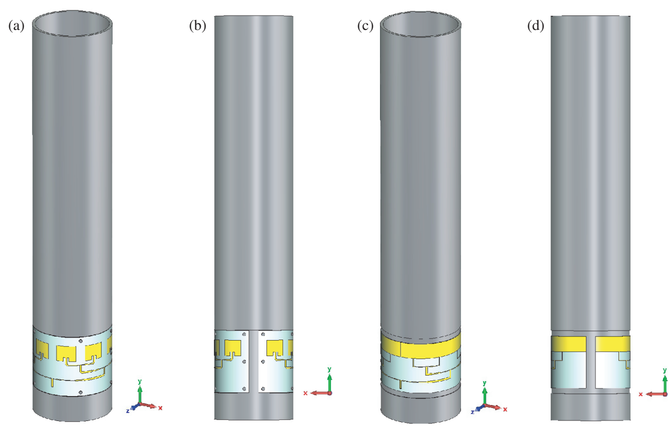

FIGURE 2. Design of conformal microstrip antennas mounted on the cylinder: RP antennas (a) front and (b) back views, as well as LP antennas (c) front and (d) back views.

noted that the impedance of 96.91 Ω is calculated using (14), while the impedances of 70.71 Ω and 69.61 Ω are the quarter wavelength transformers obtained from (5). Furthermore, the determination of the feed line lengths for each impedance values is dependent on the positioning of the rectangular patch elements. However, it is noteworthy that the 70.71 Ω and 69.61 Ω lines maintain a consistent length equivalent to $\lambda/4$. Additionally, it is important to observe that the distance between stages should be equal to one-fourth of the wavelength ($\lambda/4$).

Each of the proposed antennas is affixed to the rocket cylinder by the utilization of multiple bolts. In addition, the cylinder is composed of a material known as a perfect electrical conductor (PEC), possessing a diameter measuring 205 mm, a length of 1.04 mm, and a thickness of 7.5 mm. In the modeling of the conformal RP antenna, both the cylinder and bolts are included in order to assess their effect on the S_{11}-parameter and radiation pattern of the antennas. Fig. 2(a) illustrates the configuration of a conformal RP antenna that has been affixed to the rocket cylinder. Meanwhile, Fig. 2(c) depicts the design of the conformal LP antenna when it is mounted on the cylinder. Notably, the conformal RP and LP antenna widths are insufficient to cover the rocket cylinder circumference completely. The reason for this constraint is the maximum standard size of the materials that are commercially available, which is

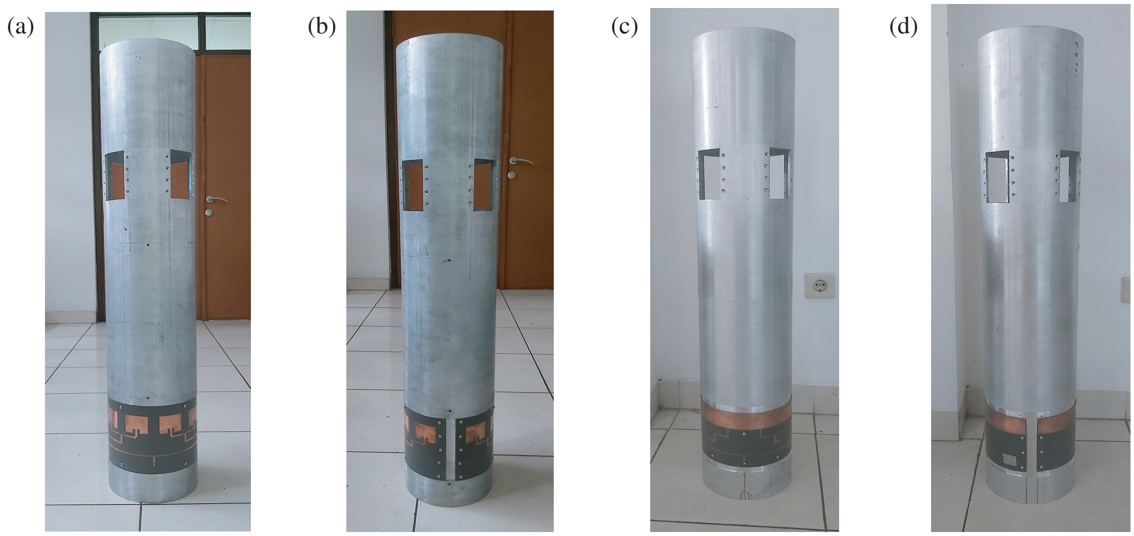

FIGURE 3. Fabricated conformal microstrip antennas mounted on the cylinder: RP antennas (a) front and (b) back views, as well as LP antennas (c) front and (d) back views.

609 mm. This size is smaller than the circumference, as depicted in Figs. 2(b) and Fig. 2(d). Nonetheless, both antenna radiation patterns cover the whole rocket cylinder circumference.

It is noteworthy to add that during the modeling of planar and conformal microstrip antennas, a significant number of meshes were employed to ensure the attainment of a precise antenna design. The process of increasing the number of meshes continues until the antenna parameters, optimized based on the S_{11} values, no longer exhibit any further shifts. The planar microstrip antenna employs a T-solver algorithm with around 3 million meshes, whereas the conformal microstrip antenna utilizes an F-solver algorithm with over 1.2 million meshes. The utilization of F-solver is strongly advised for simulating the conformal antenna mounted on the cylindrical structure of the rocket, owing to the cylindrical shape of the rocket. Hence, it is possible to achieve precise outcomes in conformal simulation compared to the actual measurements. In certain cases, it may be advantageous to conduct simulations utilizing both the T-solver and F-solver to facilitate a comparative analysis. When examining the results comparison between simulation and measurement, it is observed that the simulation utilizing T-solver exhibits a variation in the S-parameter findings.

4. SIMULATION AND FABRICATION RESULTS DISCUSSIONS

Furthermore, both proposed conformal microstrip antennas are fabricated, followed by the measurement of the parameters. The fabricated antennas are then wrapped around an aluminum rocket cylinder with an outside diameter of 203 mm, a thickness of 7.5 mm, and a height of 1.04 m. The conformal microstrip antennas are installed on the rocket cylinder, i.e., at a distance of 0.81 m from the top of the cylinder. These antennas are located close to the radio telemetry equipment. Figs. 3(a) and (b) depict the conformal RP antenna that has been physically affixed to the rocket cylinder, as observed from the front and back perspectives, respectively, while Figs. 3(c) and (d) illustrate the front and back perspectives of the manufactured conformal LP antenna, respectively. It is important to note that the section of the cylinder designated for antenna installation has undergone drilling to a depth of 1.6 mm. Consequently, the antenna is expected to remain securely attached throughout the flight test, as it will be resistant to detachment caused by the aerodynamic forces exerted by the rocket.

4.1. Antenna Performance

The S_{11} characteristics of planar and conformal RP antennas are assessed using computer simulation and field measurement, by examining a maximum reflection coefficient (S_{11}) of less than or equal to -10 dB, as depicted in Fig. 4(a). The simulation results indicate that the planar RP antenna exhibits resonance at 2.44 GHz with an S_{11} value of -31.318 dB, featuring a 48 MHz bandwidth. When the RP antenna is affixed to the cylindrical structure, creating a conformal RP antenna, its bandwidth slightly narrows to 44 MHz, while the center frequency remains fixed at 2.443 GHz with an S_{11} value upward shift to -24.39 dB. It should be emphasized that the center frequency of the conformal RP microstrip antenna is relatively identical to the planar microstrip antenna, and yet the S_{11} value is worse than the planar one.

It is observed that the S_{11}-parameter measurements of fabricated RP antenna yield values that closely align with the simulation findings for the planar RP antenna. The center frequency is measured at 2.445 GHz within a bandwidth of 50 MHz. At this center frequency, the S_{11} value is measured to be -35.075 dB. However, variations in the measurements of the conformal RP antenna installed on the rocket cylinder have been observed. These measurements indicate that the frequency remains unchanged comparable to the planar antenna, resonating at 2.445 GHz with a bandwidth of 48 MHz. Only the

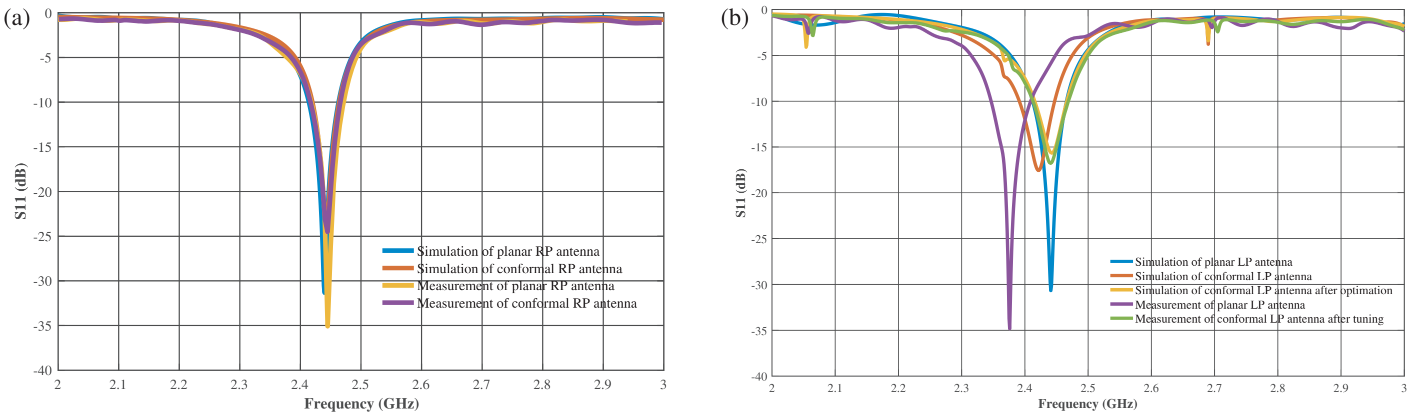

FIGURE 4. Simulation and measurement S_{11}-parameter results comparison of planar and conformal (a) RP and (b) LP antennas.

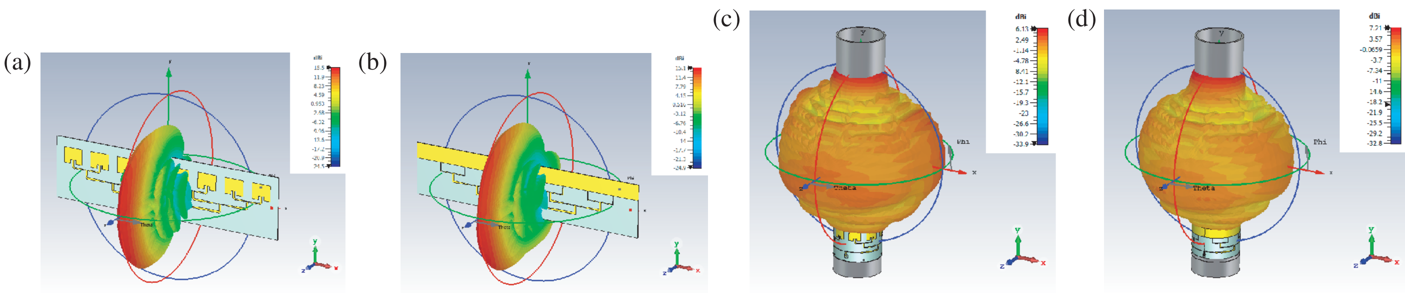

FIGURE 5. Simulation 3D radiation pattern: (a) Planar RP, (b) Planar LP, (c) Conformal RP, and (d) Conformal LP.

S_{11} value is increased, recorded as -24.512 dB. Hence, based on the obtained measurement results, it can be inferred that the cylinder of the rocket, possessing a diameter of approximately 203 mm, exerts minimal influence on the resonant frequency of the conformal RP antenna, making its effect inconsequential. It is worth mentioning that the bending of the antenna along the width of the patch does not result in any alteration of the resonant frequencies of the antenna. Similar findings have also been examined in [24] and [25].

The evaluation of various outcomes is conducted based on the S_{11}-parameter of the LP antenna, as depicted in Fig. 4(b). Based on the simulation results, it is observed that the planar LP antenna, having a length L_p of 39.9 mm, exhibits resonance at the central frequency of 2.44 GHz. The S_{11} of antenna is measured to be -30.67 dB, indicating a strong impedance match. Furthermore, the antenna demonstrates a bandwidth of 52 MHz. However, when the antenna is mounted on the rocket cylinder, the central frequency undergoes a shift to 2.42 GHz, with a bandwidth of 55 MHz. Consequently, the L_p is optimized to a length of 39.5 mm, resulting in a center frequency of 2.44 GHz. The S_{11} parameter is measured to be -15.65 dB, and the bandwidth spans 50 MHz.

The fabricated LP antenna is subjected to measurement, and the obtained results indicate that the resonant frequency of the planar LP antenna experiences a downward shift to 2.38 GHz. Nevertheless, there are notable distinctions when comparing it to the simulation. It is worth noting that the occurrence of this phenomenon can be attributed to the imprecise quality of the printing process, wherein variations in patch size result in a shift in the resonant frequency. The conformal LP antenna mounted on the rocket cylinder is adjusted by decreasing the size of the L_p to a specific value slightly above 39 mm. This adjustment is made to achieve resonance at a frequency of 2.44 GHz featuring an S_{11} value of -16.76 dB, with a bandwidth of 55 MHz. During the process of simulation and experiment, it has been observed that the resonant frequency of the conformal LP antenna is greatly influenced by the diameter of the rocket cylinder. Therefore, the decrease in diameter causes a change in the resonant frequency towards a lower frequency.

Based on the simulation results, it is shown that the planar RP antenna exhibits a directional radiation pattern, featuring a maximum gain of 15.5 dB, as shown in Fig. 5(a). Nevertheless, when the RP antenna is installed conformally around the rocket cylinder, it undergoes a transformation in its radiation pattern, resulting in an omnidirectional pattern. Consequently, this transformation reduces the maximum gain to 6.13 dB, as illustrated in Fig. 5(c). Moreover, the simulation of the LP antenna yields a comparable outcome to the aforementioned RP antenna. The planar LP antenna has a directional radiation pattern with a maximum gain of 15.1 dB, as shown in Fig. 5(b). After the antenna is mounted around the rocket cylinder, the radiation pattern turns into an omnidirectional pattern, leading to a decrease in the maximum gain to 7.21 dB, as depicted in Fig. 5(d). Due to the constrained standard dimensions of the material, the patch elements in our design do not span the entire circumference of the rocket cylinder. Nonetheless, the radi-

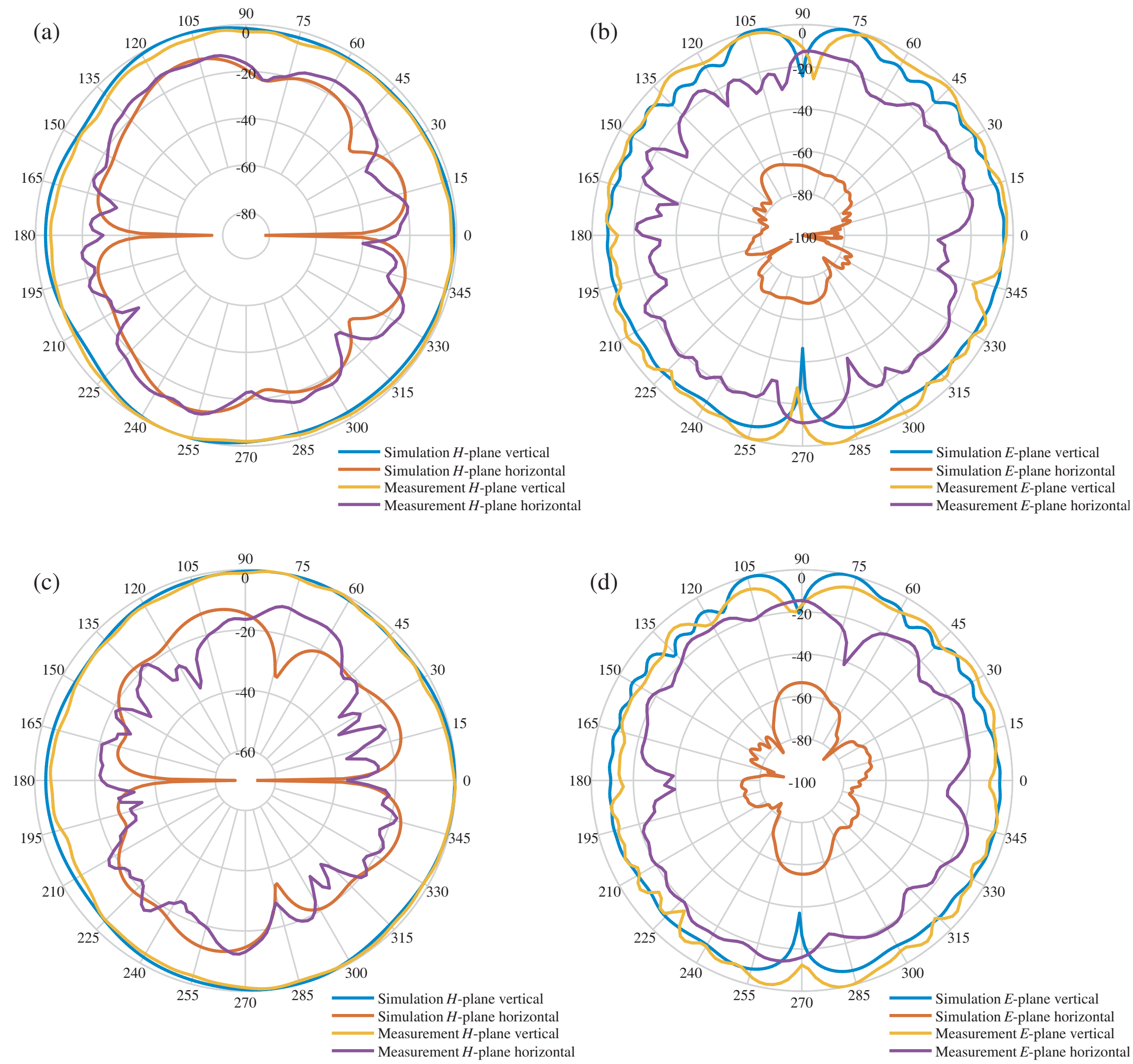

FIGURE 6. Normalized radiation pattern of conformal antennas mounted on the cylinder from simulation and measurement: (a) H-plane RP antenna, (b) E-plane RP antenna, (c) H-plane LP antenna, and (d) E-plane LP antenna.

ation pattern remains omnidirectional. Furthermore, to provide a toroidal radiation pattern with uniform coverage in all directions, it is necessary for the patch array elements of conformal RP antennas to maintain equal spacing between each other. Alternatively, for conformal LP antennas, the single patch element should be designed to match the circumference of a cylinder.

In addition, the radiation characteristics of the fabricated conformal RP and LP antennas, which are installed on the cylindrical structures, are evaluated within the *semi*-anechoic chamber located at the Electromagnetic Compatibility (EMC) Laboratory of the Research Center for Electronics, BRIN. The radiation patterns of conformal RP and LP antennas are illustrated in Fig. 6. These patterns are based on gain values that have been normalized to 0 dB. It is important to note that both simulation and measurement data are utilized to generate these plots. The radiation patterns of the H-plane vertical and E-plane vertical demonstrate that conformal RP and LP antennas have an omnidirectional radiation pattern. Nevertheless, the radiation patterns of H-plane horizontal and E-plane horizontal exhibit a nearly omnidirectional radiation pattern with minimal sidelobes and lower gain values than their vertical counterparts. It should be noted that the measured radiation pattern demonstrates a resemblance to the results obtained from the simulation. However, the simulated E-plane horizontal exhibits significantly lower gain values than its corresponding measured radiation pattern, which is still under investigation. Moreover, the radiation pattern of antennas in the E-plane indicates that the presence of a metallic cylinder leads to the formation of multiple maxima lobes.

Furthermore, the determination of the polarization of the conformal microstrip antenna is reliant on its axial ratio, as stated in [19]. Figs. 7(a) and 7(b) illustrate the polar plot simulation of the axial ratio at a specific azimuthal angle of $\phi = 0°$ for the conformal RP and LP antennas, respectively. The presented data demonstrates that the axial ratio values of both antennas

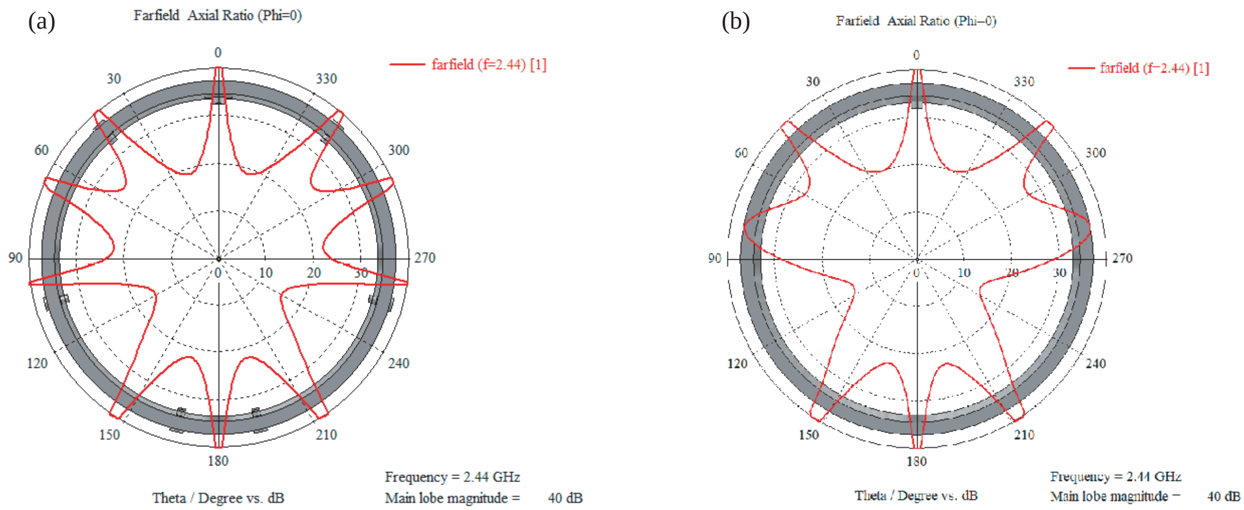

FIGURE 7. Polarization of Conformal (a) RP Antenna and (b) LP Antenna.

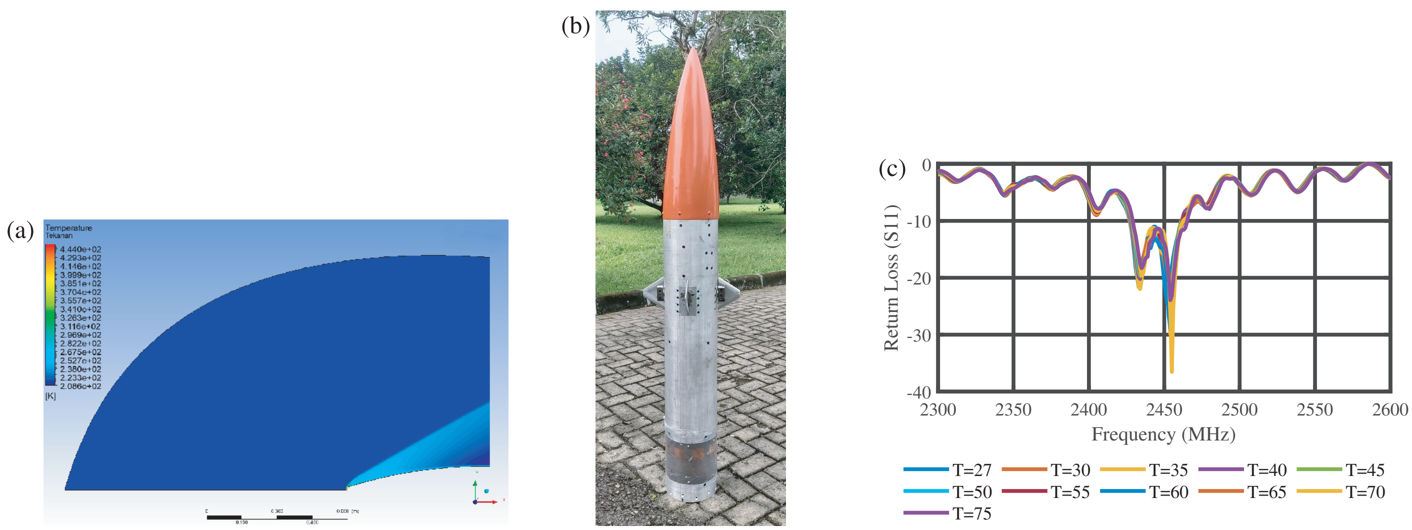

FIGURE 8. (a) CFD simulation of the rocket-nose cone, (b) Rocket cylinder with installed nose cone, and (c) S_{11} parameter over different temperature.

exhibit a range spanning from 10 dB to 40 dB. Hence, it can be observed that both the conformal RP and LP antennas exhibit linear polarization. Additionally, the assessment of the gain values of the antennas in vertical and horizontal polarizations indicates that both antennas demonstrate vertical polarization.

4.2. Thermal Distribution

The temperature of the surrounding air is one of the factors that influences the performance of the antenna mounted on the rocket outer body. Due to their speed and altitude, rockets flying through the atmosphere encounter temperature variations. Therefore, we must make sure that the proposed antenna is not utilized in the atmosphere over the prescribed temperature. Besides, as mentioned in [26], antenna performance decreases with rising ambient temperature. One might observe such effects by looking at the particular thermal coefficient of ϵ_r or the coefficient of thermal expansion of the roger material described in [27].

Simulating the thermal distribution on the rocket's outer body (diameter: 203 mm) during flight tests is crucial, especially where the conformal microstrip antenna will be placed. A 2D Computational Fluid Dynamics (CFD) simulation of the rocket's aft-nose cone is illustrated in Fig. 8(a), and the nose cone installed on the rocket cylinder with a mounted conformal RP antenna is captured in Fig. 8(b). In Fig. 8(a), the temperature on the aft-nose cone ranges from 286°K to 345°K [28, 29]. The thermal simulation indicates that the antenna will experience a maximum heat exposure of approximately 345°K or 71.8°C immediately after the nose cone. Furthermore, as we move further away from the tip of the nose cone, the temperature decreases, and the maximum heat exposure around the conformal microstrip antenna remains lower, below the melting temperature of the Roger material used. Consequently, our proposed antenna can endure high-temperature conditions during flight tests. Moreover, it is essential to explore the impact of temperature fluctuations on antenna bandwidth in this research.

TABLE 1. Temperature effect on the antenna.

Temperature (°C)	Calculation			Measurement		
	ε_r	L_p (mm)	f_r (GHz)	f_r (GHz)	S_{11}	BW (MHz)
27	2.2000	41.0000	2.4520	2.452	-24.547	34
30	2.1992	41.0059	2.4521	2.453	-23.353	33
35	2.1978	41.0157	2.4532	2.454	-29.893	33
40	2.1964	41.0256	2.4525	2.455	-29.705	33
45	2.1952	41.0354	2.4526	2.454	-25.969	32
50	2.1937	41.0453	2.4528	2.455	-31.535	33
55	2.1923	41.0551	2.4530	2.455	-30.846	32
60	2.1909	41.0650	2.4532	2.455	-29.246	34
65	2.1896	41.0748	2.4534	2.455	-27.321	34
70	2.1882	41.0847	2.4535	2.455	-36.546	32
75	2.1868	41.0946	2.4537	2.454	-23.952	35

The impact of heat exposure on the conformal antenna mounted on the rocket cylinder tube assessed through CFD simulation is then evaluated in the measurements. Table 1 compares the calculated and measured temperature-dependent behaviors of the conformal antenna. In the calculation, changes in the center frequency resulting from temperature fluctuations are determined using (17) with known values of α_{ε_r} and α_L along the antenna material length, as detailed in [27]. We obtain that the calculated center frequency is observed to increase with rising temperatures. On the other hand, the measurements are conducted in the thermal chamber (VÖTSCH VC4018) of the Research Center for Satellite Technology BRIN. The antenna installed on a cylinder is placed in the thermal chamber and exposed to temperature ranges from 27°C to 75°C, following the CFD simulation temperature. Subsequently, the S_{11} values of the antenna are measured using a vector network analyzer (VNA) connected to the antenna through a coaxial cable. The result demonstrates that the central frequency increases as the temperature rises. The results confirm that the center frequency shifts very slightly about 1–2 MHz to a higher frequency as the temperature increases, consistent with the calculations. Meanwhile, the bandwidth of the conformal RP antenna obtained from the thermal measurement can be seen in Fig. 8(c). It remains relatively stable across different temperatures, with slight variations. This suggests that the temperature changes do not significantly impact the antenna's ability to operate within a certain frequency range.

5. CONCLUSION

This paper provides the analysis through simulation and fabrication measurement results regarding two types of conformal microstrip antennas mounted on a rocket cylinder, i.e., conformal RP and LP antennas. The results denote that the proposed conformal RP antenna resonates at the center frequency of 2.445 GHz featuring a bandwidth of 48 MHz. In addition, the conformal LP antenna has a resonant frequency of 2.44 GHz with a wider bandwidth of 55 MHz. It should be noted that the resonant frequency of the conformal RP antenna is not specifically affected by the utilization of a rocket cylinder with a diameter of 203 mm. On the other hand, the resonant frequency of the conformal LP antenna is quite affected by the utilization of the rocket cylinder, particularly by its diameter. Moreover, our conformal RP and LP antennas mounted on the cylinder exhibit an omnidirectional radiation pattern with a maximum gain of 6.13 dB and 7.21 dB, respectively. Meanwhile, the proposed conformal antennas are still working with a good performance during the flight test until a maximum temperature exposure of 71.8°C. Finally, it can be resumed that the measurement results exhibit a very good agreement compared to the simulation results.

ACKNOWLEDGEMENT

This research is funded by the Research Program of National Research and Innovation Agency (BRIN), entitled The Development of Conformal Antennas for Rocket Telemetry Systems (Grant No. 1/III.1/HK/2023). Also, we wish to acknowledge and thank the support of Maksum Sumantri, Hery Suwarto, Sutisna, Slamet Subagyo, A.Md. from PRTR BRIN in the fabrication and measurements of the antenna, as well as Dr. Ir. Reza Septiawan from PRE BRIN for antenna measurements in the anechoic chamber.

REFERENCES

[1] Chelstowski, T., K. Dobrzyniewicz, P. Kant, and J. J. Michalski, "Long range radio location system employing autonomous tracking for sounding rocket," in *2018 22nd International Microwave and Radar Conference (MIKON)*, 400–403, 2018.

[2] Jansen, I. S., R. Maximidis, M. Wijtvliet, and A. B. Smolders, "Design and evaluation of a radio-interferometry antenna for the REXUS 25 sounding rocket," in *2020 14th European Conference on Antennas and Propagation (EuCAP)*, 1–5, 2020.

[3] Sripho, P., S. Duangsi, and M. Hongthong, "Comparison of antenna for DTI rocket telemetry system," in *2016 Second Asian Conference on Defence Technology (ACDT)*, 105–110, 2016.

[4] Prades, J., A. Ghiotto, E. Kerhervé, and K. Wu, "Broadband sounding rocket antenna for dual-band telemetric and payload data transmission," *IEEE Antennas and Wireless Propagation Letters*, Vol. 15, 540–543, 2016.

[5] Pascawati, A., P. Hazdra, T. Lonsky, and M. R. K. Aziz, "Excitation of a conducting cylinder using the theory of characteristic modes," *Radioengineering*, Vol. 27, No. 4, 956–960, 2018.

[6] Pascawati, A., K. Rahardiyanti, M. Fakhri, A. Riyadl, E. Artono, Kurdianto, and M. R. K. Aziz, "Blade antenna 2.4 GHz for rocket applications," in *2021 International Conference on Computer System, Information Technology, and Electrical Engineering (COSITE)*, 204–208, 2021.

[7] Ribeiro Filho, P. C., A. F. Tinoco-S., D. C. Nascimento, and J. C. D. S. Lacava, "A telemetry antenna design for a sounding rocket competition [antenna applications corner]," *IEEE Antennas and Propagation Magazine*, Vol. 59, No. 3, 100–140, 2017.

[8] Tang, M.-C., Y. Duan, Z. Wu, and M. Li, "Flexible, conformal, endfire radiating, electrically small antennas on a conducting cylinder with a small radius," *IEEE Transactions on Antennas and Propagation*, Vol. 68, No. 5, 3496–3503, 2020.

[9] Beaskoetxea, U., J. C. Iriarte, I. Ederra, I. Maestrojuan, and M. Melara, "Design of multiband conformal antenna for sounding rocket," in *2020 14th European Conference on Antennas and Propagation (EuCAP)*, 1–3, 2020.

[10] Bhattacharya, D., B. Ghosh, and K. Sarabandi, "Evaluation of efficient closed-form Green's function in a cylindrically stratified medium," *IEEE Transactions on Antennas and Propagation*, Vol. 65, No. 3, 1505–1510, 2017.

[11] Bhattacharya, D., B. Ghosh, P. K. Goswami, and K. Sarabandi, "Evaluation of efficient Green's functions for spherically stratified media," *IEEE Transactions on Antennas and Propagation*, Vol. 66, No. 3, 1613–1618, 2018.

[12] Ghosh, B., K. Chakraborty, G. Santra, and K. Sarabandi, "Loop excitation of a conical horn," *IEEE Transactions on Antennas and Propagation*, Vol. 66, No. 6, 2727–2740, 2018.

[13] Ghosh, B., S. K. M. Haque, and P. Halder, "Analysis of arbitrary multiple-loop antennas around a conducting cone, with rotational symmetry," *IET Microwaves, Antennas & Propagation*, Vol. 7, No. 2, 111–122, 2013.

[14] Halder, P., B. Ghosh, S. K. M. Haque, and K. Sarabandi, "Loop antenna over a conducting cone with a spherical cap," *IET Microwaves, Antennas & Propagation*, Vol. 13, No. 14, 2559–2568, 2019.

[15] Jaglan, N., S. D. Gupta, and M. S. Sharawi, "18 element massive MIMO/diversity 5G smartphones antenna design for sub-6 GHz LTE bands 42/43 applications," *IEEE Open Journal of Antennas and Propagation*, Vol. 2, 533–545, 2021.

[16] Jaglan, N., S. D. Gupta, B. K. Kanaujia, and M. S. Sharawi, "10 element sub-6-GHz multi-band double-T based MIMO antenna system for 5G smartphones," *IEEE Access*, Vol. 9, 118 662–118 672, 2021.

[17] Thakur, V., N. Jaglan, and S. D. Gupta, "Side edge printed eight-element compact MIMO antenna array for 5G smartphone applications," *Journal of Electromagnetic Waves and Applications*, Vol. 36, No. 12, 1685–1701, 2022.

[18] Pascawati, A., M. Fakhri, M. Z. Rahmat, I. E. Putro, R. A. Duhri, S. D. Harsono, H. Y. Irwanto, Y. Wahyu, B. Sulistya, A. Rufiyanto, and M. R. K. Aziz, "Conformal microstrip rectangular patch array 8×1 antenna for rocket," in *AIP Conference Proceedings*, Vol. 2941, No. 1, 020059, 2023.

[19] Balanis, C. A., *Antenna Theory: Analysis and Design*, John Wiley & Sons, 2016.

[20] Munson, R., "Conformal microstrip antennas and microstrip phased arrays," *IEEE Transactions on Antennas and Propagation*, Vol. 22, No. 1, 74–78, 1974.

[21] Harrington, R. F., *Time-Harmonic Electromagnetic Fields*, IEEE Press, 2001.

[22] Tchafa, F. M. and H. Huang, "Microstrip patch antenna for simultaneous strain and temperature sensing," *Smart Materials and Structures*, Vol. 27, No. 6, 065019, May 2018.

[23] Narasagond, S., C. Jayanth, and S. Vedagarbham, "A comparison between inset feed and proximity feed techniques for MSA," in *2018 3rd IEEE International Conference on Recent Trends in Electronics, Information & Communication Technology (RTEICT)*, 228–231, 2018.

[24] Patil, S., M. Ar, C. Sudhendra, R. Ts, and D. Biswas, "Design and implementation of a conformal omnidirectional microstrip antenna array on cylindrical surface," *International Journal of Advances in Electronics and Computer Science*, 2393–2835, 2015.

[25] Song, L. and Y. Rahmat-Samii, "A systematic investigation of rectangular patch antenna bending effects for wearable applications," *IEEE Transactions on Antennas and Propagation*, Vol. 66, No. 5, 2219–2228, 2018.

[26] Yadava, R. L., *Antennas and Wave Propagation*, PHI Learning Private Limited, 2022.

[27] Rogers Corporation, "RT/duroid® 5870 and 5880 high frequency laminates," 2022. [Online]. Available: https://www.rogerscorp.com/-/media/project/rogerscorp/documents/advanced-electronics-solutions/english/data-sheets/rt-duroid-5880lz-high-frequency-laminates.pdf.

[28] Putro, I. E., "Rocket design," Tech. Rep. TD-11/GL1/PTR/VIII/2021, National Institute of Aeronautics and Space (LAPAN), 2021.

[29] Duhri, R. A., "Perhitungan CFD Nosecone RX-200," Tech. Rep. TN-01/ES1.1.2/ROKET/VIII/2021, National Institute of Aeronautics and Space (LAPAN), 2021.